A New Species of *Chromis* (Teleostei: Pomacentridae) from Mesophotic Coral Ecosystems of Rapa Nui (Easter Island) and Salas y Gómez, Chile

Bart Shepherd[1], Hudson T. Pinheiro[2], Tyler A. Y. Phelps[2,3], Erin E. Easton[4,5], Alejandro Pérez-Matus[6], and Luiz A. Rocha[2]

A new species of *Chromis* (Teleostei: Pomacentridae) is described from three specimens collected at 90 m depth in a mesophotic coral ecosystem at Rapa Nui, Chile. *Chromis mamatapara,* new species, can be distinguished from its congeners by the following combination of characters: dorsal-fin rays XIV,13–14; pectoral-fin rays 18–19, third from top of fin longest; tubed lateral-line scales 18; total gill rakers on first arch 30–32; vertebrae 11+15; and by coloration of living specimens, especially the presence of a single, pronounced, white spot, roughly the same diameter as the orbit, located where the posterior base of the dorsal fin intersects the caudal peduncle. The most similar DNA barcode (mitochondrial *COI* gene), among those available, is *Chromis tingting* from Japan (3.5% uncorrected divergence); however, *C. mamatapara,* new species, also superficially resembles other species for which sequences are unavailable for comparisons, including *C. okamurai* from Japan and *C. struhsakeri* from Hawaii. Due to the high geographic isolation and consequently high endemism in the Rapa Nui region, we believe that *C. mamatapara*, new species, is endemic to mesophotic ecosystems of Rapa Nui, Isla Salas y Gómez, and nearby seamounts, a discovery that contributes to the high endemism of the region and thus the need for conservation efforts.

THE more than 400 described species within the Pomacentridae (damselfishes and anemonefishes), one of the largest families of reef fishes, exhibit a wide range of morphologies and occupy multiple ecological niches (Allen, 1991; Muñoz-Cordovez et al., 2019). Fishes within the genus *Chromis* are predominantly planktivores, and several studies have shown that their relative abundance increases with depth (Thresher and Colin, 1986; Bejarano et al., 2014; Pinheiro et al., 2016; Coleman et al., 2018). *Chromis* is the most species-rich genus within the Pomacentridae, comprising more than 100 valid species, at least ten of which, including several recently described species, are found only below 60 m (Pyle et al., 2008; Allen and Erdmann, 2012; Arango et al., 2019; Tea et al., 2019). They are conspicuous residents of mesophotic coral ecosystems (MCEs, coral reef habitats occurring at depths from 30–150 m) across the Pacific, and are often seen in high numbers where they occur.

Rapa Nui (Easter Island) is one of the most isolated islands in the world, located approximately 3,700 km west of Chile and 2,000 km from the nearest inhabited island, Pitcairn (Randall and Cea, 2010; Easton et al., 2017). The Rapa Nui fish fauna exhibits a very low overall diversity (Friedlander et al., 2013; Easton et al., 2017); nevertheless, it presents the second-highest endemism in both shallow-water and deep-sea fishes in the Indo-Pacific, with nearly 22% of the shore fishes being endemic (Randall and Cea, 2010; Friedlander et al., 2013). Recent genetic studies have revealed that Rapa Nui is an endemism hotspot: a location for the emergence of small-range endemic fishes (likely resulting from founder-event speciation), a route of dispersion for larger-range endemics, and a stepping stone for the diversification of some groups (Delrieu-Trottin et al., 2019).

Easton et al. (2019) provided a thorough summary of the historical surveys conducted in the Rapa Nui and Isla Salas y Gómez ecoregion. Although ichthyological surveys in the area date back to the early twentieth century, there have been relatively few surveys of fish communities living at depths greater than 40 m (Easton et al., 2019). Those that have occurred indicate that species richness is surprisingly high on MCEs, but overall MCE fish diversity at Rapa Nui remains unknown (Friedlander et al., 2013; Wieters et al., 2014; Easton et al., 2017, 2019). This combination of isolation, speciation from founder events, and lack of exploration makes Rapa Nui a fascinating location to study the biodiversity of MCEs and its links to that of shallow reefs.

Through a partnership between the Pontificia Universidad Católica de Chile and the Hope for Reefs Initiative of the California Academy of Sciences, our team conducted surveys to depths of 110 m to describe and identify the fish communities associated with MCEs at Rapa Nui. These led to the collection of several new species, two of which have been recently described (Shepherd et al., 2018a, 2019). Here, we describe a third new species of fish resulting from these surveys, a damselfish of the genus *Chromis* (Teleostei: Pomacentridae), collected at 90 m on a rocky mesophotic ecosystem in March 2017.

MATERIALS AND METHODS

Meristics, morphometrics, and specimen deposition.—Specimens were collected and immediately transported to a field

[1] Steinhart Aquarium, California Academy of Sciences, San Francisco, California 94118; Email: bshepherd@calacademy.org. Send reprint requests to this address.
[2] Department of Ichthyology, California Academy of Sciences, San Francisco, California 94118.
[3] Department of Biology, San Francisco State University, San Francisco, California 94132.
[4] Ecology and Sustainable Management of Oceanic Islands, Universidad Católica del Norte, Coquimbo, Chile.
[5] Present address: School of Earth, Environmental and Marine Sciences, University of Texas Rio Grande Valley, Brownsville, Texas 78520.
[6] Subtidal Ecology Laboratory, Estación Costera de Investigaciones Marinas, Facultad de Ciencias Biológicas, Pontificia Universidad Católica de Chile, Casilla 114-D, Santiago, Chile.

laboratory, where they were photographed, tissue sampled, and fixed in 10% formalin. Measurements and x-radiographs were made at the California Academy of Sciences more than two years after fixation and followed by preservation in 75% ethanol. Counts were performed with the aid of a microscope; measurements were made with digital calipers to the nearest 0.01 mm and rounded to one decimal place, following the conventions described in Allen and Randall (2004) and Pyle et al. (2008). Spiniform procurrent caudal-fin rays are those situated anteriorly to segmented procurrent caudal-fin rays, especially visible in radiographs. Vertebral counts include the first vertebra fused to the skull, and the last vertebra fused to the hypural plate; vertebral counts are presented as precaudal + caudal, where the first caudal vertebra is the anterior-most vertebra having its haemal spine associated with the anal fin pterygiophore, and the last caudal vertebra is fused to the hypural plate. Gill-raker counts are presented as upper (epibranchial) + lower (ceratobranchial) rakers on the anterior face of the first arch; the angle raker is included in the second count. Morphometric and meristic data for the holotype and paratypes are presented in Table 1. Measurements in the text are proportions of standard length (SL), unless otherwise noted. Data are presented first for the holotype, followed by a range of values for the paratypes, in parenthesis, where variation was noted. The holotype and paratypes were deposited at the California Academy of Sciences (CAS) and Smithsonian Institution, National Museum of Natural History (USNM) ichthyological collections.

Taxon sampling, sequencing, and genetic comparisons.—This species was first photographed in Drop-Cam surveys at Isla Salas y Gómez at 150 m and ROV (remotely operated vehicle) surveys at Rapa Nui at 157–171 m but not collected (Easton et al., 2017: fig. 4D). In March 2017, three individuals were collected with Hawaiian sling by members of our team diving on mixed-gas, closed-circuit rebreathers (Hollis Prism 2). Molecular analysis and PCR amplification of the standard barcode fragment of the mitochondrial cytochrome c oxidase subunit I gene (*COI*) were performed following protocols described by Arango et al. (2019) using BOLFishF1/BOLFishR1 primers. Alignments of DNA sequences were done using a standard Geneious global alignment with free end gaps and 65% similarity in the program Geneious Prime 2020.0.3 (Kearse et al., 2012). Because taxon sampling for *Chromis* in public databases and our lab is not very high, and we only sequenced one mitochondrial DNA marker, we did not attempt to perform a phylogenetic reconstruction. For our comparisons, genetic distances are uncorrected. We used all available *COI* sequences of *Chromis* from GenBank (63 species, Supplemental Table 1; see Data Accessibility) for genetic comparisons.

Chromis mamatapara, new species

urn:lsid:zoobank.org:act:9A0A722B-391C-44C8-A534-16ACA5DFF4C6
GenBank identifier for holotype: MN708011
English Common Name: Michel's Chromis
Spanish Common Name: Castañeta de Michel
Figures 1–3, Table 1

Holotype.—(Figs. 1, 3) CAS 247107 (field code LAR2650), 114.6 mm SL, Rapa Nui (Easter Island), Chile, Hanga Piko, 27°9′12″S, 109°26′52″W, Hawaiian sling, depth of collection 90 m, Luiz Rocha, Tyler Phelps, Mauritius Bell, 11 March 2017.

Paratypes.—CAS 247108 (field code LAR2648), 105.3 mm SL; USNM 447900 (field code LAR2649), 108.7 mm SL (both collected with holotype).

Diagnosis.—The following combination of characters distinguishes *Chromis mamatapara,* new species, from all of its congeners: dorsal-fin rays XIV (versus XV in *C. randalli,* the only other congener in the area, and XII–XIII or XV in most other Indo-Pacific species), 13–14 (versus 10 in *C. randalli*); anal-fin rays II,12 (versus II,10–11 in *C. randalli*); pectoral-fin rays 18–19 (versus 21–22 in *C. randalli*); principal caudal-fin rays 8+7; spiniform procurrent caudal-fin rays 2; tubed lateral-line scales 18 (versus 21–22 in *C. randalli*); posterior, mid-lateral scales with pore or deep pit 8–9; vertebrae 11+15; gill rakers 9–10+21–23; total gill rakers 30–32 (versus 33–37 in *C. randalli*); body moderately deep, depth 1.8–2.0 in SL (versus 2.3–3.0 in *C. randalli*); tail and caudal peduncle yellow; distal edge of caudal peduncle at junction of posterior dorsal fin with a large white spot, its diameter about width of orbit (Fig. 1).

Description.—Dorsal-fin rays XIV,13 (XIV,13–14); anal-fin rays II,12; all soft dorsal- and anal-fin rays branched, the last to base, the last two soft rays associated with a single complex pterygiophore; sixth dorsal ray longest, 5.7 in SL (4.7–5.5); pectoral-fin rays 18|18 (18–19|18), the uppermost and lowermost unbranched (uppermost two and lowermost in paratypes); pectoral-fin ray 3.2 in SL (3.0–3.1), the third ray longest; pelvic-fin rays I,5; principal caudal-fin rays 8+7, the uppermost and lowermost unbranched; upper and lower procurrent caudal-fin rays 4, the anteriormost 2 rays (dorsally and ventrally) spiniform; tubed lateral-line scales 18 (damaged on left side in holotype); posterior midlateral scales with a pore 8 (8–9); scales above lateral line to origin of dorsal fin 3; scales below lateral line to origin of anal fin 11 (10–11); circumpeduncular scales 15 (14); gill rakers 9+23 = 32 (9–10+21 = 30–31); supraneural bones 3; vertebrae 11 precaudal + 15 caudal = 26.

Body moderately deep, depth 2.0 (1.8–2.0) in SL, and compressed, the width 2.7 in body depth; head length 3.4 (2.9–3.2) in SL; profile of head slightly convex above orbit, nape slightly convex; snout length 4.5 (3.3–3.6) in head length; orbit diameter 2.7 (3.1–3.2) in head length; interorbital width 2.7 (2.8–3.3) in head length; caudal-peduncle depth 2.1 (2.3) in head length; caudal-peduncle length 2.3 (2.2–2.3) in head length.

Mouth terminal, oblique, upper jaw angle about 35° to the horizontal axis of head and body; posterior edge of maxilla vertical at anterior edge of pupil, upper jaw length 3.5 (3.3–3.9) in head length; teeth multi-serial, outer row of conical teeth in each jaw, largest anteriorly; narrow band of villiform teeth lingual to outer row, in five irregular rows anteriorly, narrowing to a single row on side of jaws; tongue triangular with rounded tip; gill rakers long and slender, longest on lower limb near angle almost the same length as gill filaments; anterior nostril with a short fleshy rim, more elevated on posterior edge and located at level of horizontal line through middle of pupil, slightly less than halfway between front of snout and anterior edge of orbit; posterior nostril smaller and slit-shaped, located just above and behind

Table 1. Counts and measurements for the holotype and paratypes of *Chromis mamatapara*, new species. All proportional measurements are presented as a percentage of standard length, unless otherwise indicated. Field numbers (LAR prefix) are given beside collection catalog numbers. Values separated by a vertical slash are presented as left|right.

	Holotype	Paratypes	
	CAS 247107 (LAR2650)	CAS 247108 (LAR2648)	USNM 447900 (LAR2649)
TL (mm)	149.9	142.0	146.9
Standard length (mm)	114.6	105.3	108.7
Counts			
Dorsal-fin rays	XIV, 13	XIV, 14	XIV, 13
Anal-fin rays	II, 12	II, 12	II, 12
Pectoral-fin rays	18|18	19|18	18|18
Pelvic-fin rays	I, 5	I, 5	I, 5
Principal caudal rays	8+7	8+7	8+7
Segmented procurrent caudal rays	2+2	2+2	2+2
Spiniform procurrent caudal rays	2+2	2+2	2+2
Tubed lateral-line scales	18	18	18
Posterior mid-lateral pored scales	8	8	9
Scales above l.l.	3	3	3
Scales below l.l.	11	11	10
Circumped. scales	15	14	14
Gill rakers	23+9	21+9	21+10
Supraneural bones	3	3	3
Vertebrae	26 (11+15)	26 (11+15)	26 (11+15)
Measurements			
Body depth	50.2	56.9	50.9
Body width	18.2	21.2	19.0
Head length	29.5	34.8	31.2
Snout length	6.6	10.4	8.7
Orbit diameter	10.8	11.2	9.6
Interorbital width	10.8	10.6	11.0
Caudal-peduncle depth	14.2	14.9	13.6
Caudal-peduncle length	12.8	16.0	13.5
Upper jaw length	8.5	8.9	9.4
Predorsal length	39.3	42.2	39.7
Spinous dorsal-fin base	47.8	51.9	52.0
Soft dorsal-fin base	15.5	17.8	16.6
1st dorsal spine	9.8	8.7	8.7
2nd dorsal spine	12.2	12.8	13.9
3rd dorsal spine	16.1	14.9	17.3
4th dorsal spine	16.9	16.5	18.5
5th dorsal spine	17.1	15.2	19.0
6th dorsal spine	16.9	16.5	18.7
Last dorsal spine	13.2	13.0	13.9
Longest dorsal ray	17.4 (6th)	21.4 (6th)	18.3 (6th)
Preanal length	70.3	67.6	65.9
1st anal spine	6.5	6.2	6.6
2nd anal spine	19.4	19.0	18.9
Longest anal ray	19.2 (1st)	20.8 (2nd)	17.5 (6th)
Anal-fin base	23.6	23.2	24.5
Caudal-fin length	32.3	36.8	34.1
Caudal concavity	16.2	19.2	14.0
Longest pectoral ray	30.8 (3rd)	33.5 (3rd)	32.4 (3rd)
Prepelvic length	43.2	45.9	39.3
Pelvic-spine length	17.5	19.5	18.3
1st pelvic soft ray	27.1	31.2	29.0

anterior nostril, close to edge of orbit (Fig. 3). Opercle ending posteriorly in flat spine, the tip relatively acute and not obscured by large scale; preopercular margin smooth, posterior margin extending dorsally to almost level of upper edge of orbit; suborbital with free lower margin extending nearly to a vertical at posterior edge of orbit.

Scales finely ctenoid; lateral line ending beneath rear portion of spinous dorsal fin (12th dorsal-fin spine); head scaled except lips; squamation of preorbital and suborbital regions shown in detail in Figure 3; scaly sheath at base of dorsal and anal fins, progressively thicker on soft portion; column of scales on each membrane of dorsal fin, narrowing
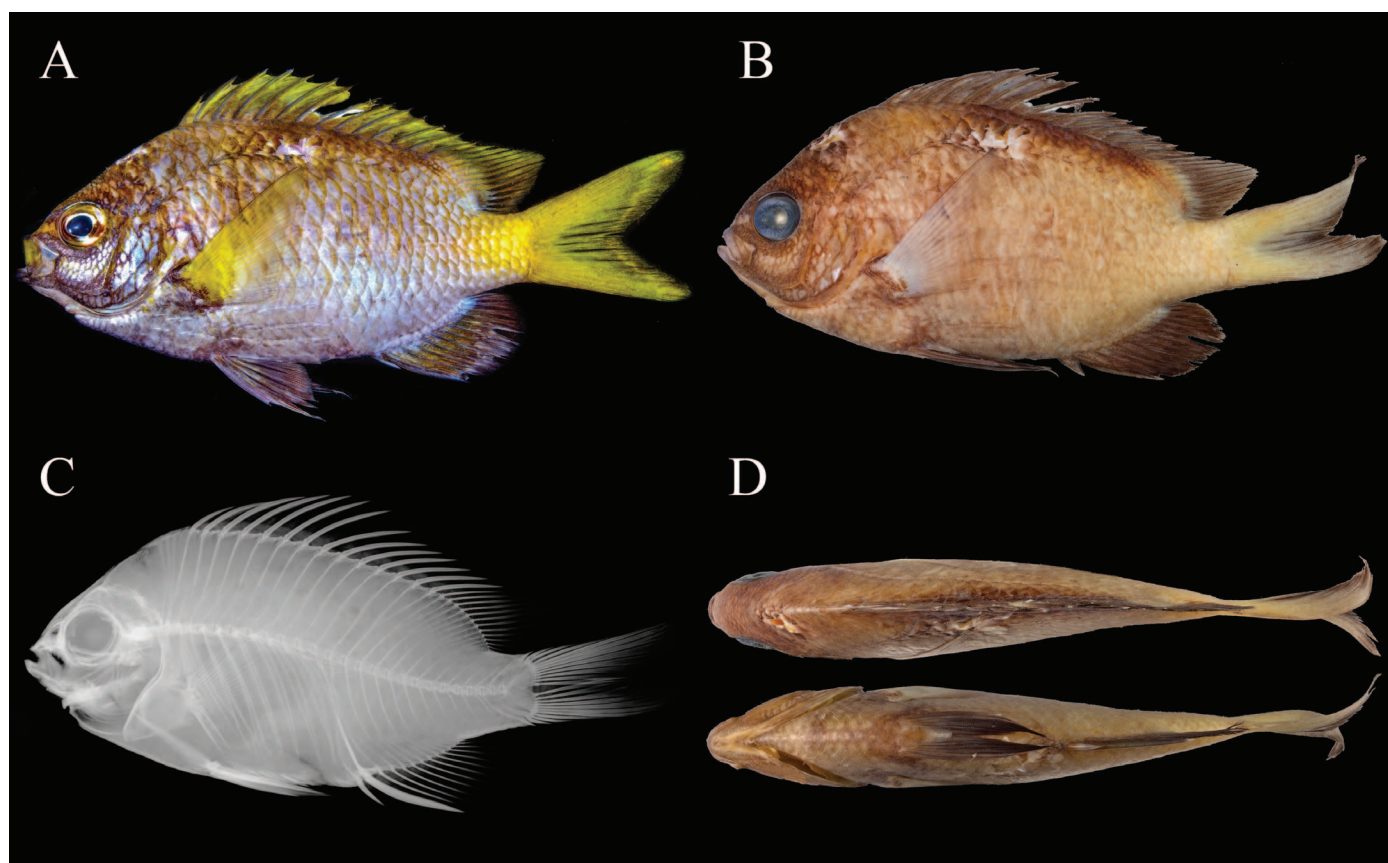
Fig. 1. (A) Holotype of *Chromis mamatapara*, new species (CAS 247107), shortly after death. Photo by L. A. Rocha. (B) Preserved holotype, lateral view. Photo by J. Fong. (C) Radiograph of holotype (CAS 247107). Photo by J. Fong. (D) Preserved holotype, dorsal and ventral views. Photos by J. Fong.

distally, those on spinous portion of dorsal fin progressively longer, reaching about half the distance to spine tips on posterior membranes; single column of scales on anal-fin membrane, progressively smaller distally; small scales on caudal fin extending almost to posterior margin; small scales on basal one-fifth of pectoral fins; median scaly process extending posteriorly from between bases of pelvic fins, its length about half that of pelvic spine; axillary scale above base of pelvic spine about half the length of pelvic spine. Origin of dorsal fin over third lateral-line scale; pre-dorsal length 2.5 (2.4–2.5) in SL; spinous dorsal-fin base length 2.1 (1.9) in SL; soft dorsal-fin base length 6.5 (5.6–6.0) in SL; first dorsal spine 10.2 (11.5) in SL; second dorsal spine 8.2 (7.2–7.8) in SL; third dorsal spine 6.2 (5.8–6.7) in SL; fourth dorsal spine 5.9 (5.4–6.0) in SL; fifth dorsal spine 5.8 (5.3–6.6) in SL; sixth dorsal spine 5.9 (5.4–6.1) in SL; last dorsal spine 7.6 (7.2–7.7) in SL; sixth dorsal ray longest, 5.7 (4.7–5.5) in SL; first anal spine 15.4 (15.1–16.2) in SL; second anal spine 5.2 (5.3) in SL; longest anal-fin ray variable, first in holotype, second and sixth in paratypes; caudal fin forked, without filamentous extensions, its length 3.1 (2.7–2.9) in SL, and concavity 6.2 (5.2–7.2) in SL; third pectoral-fin ray longest, 3.2 (3.0–3.1) in SL; pelvic spine 5.7 (5.1–5.5) in SL; first pelvic soft ray 3.7 (3.2–3.4) in SL.

Coloration of adults in life.—Recently dead adult specimens (Fig. 1A) body overall metallic pale blue to lavender; base of dorsal fin, upper third of body, and head above and behind orbit predominantly golden-brown; posterior margins of scales with yellow highlights, especially pronounced on head and dorsal two-thirds of body; upper jaw pale yellow; iris yellow, faint yellow bar through interorbital space, middle of orbit and across operculum; distal margin of dorsal fin, pectoral fins, caudal peduncle and caudal fin predominantly yellow; pelvic fins and anal fin predominantly golden-brown with pale yellow between fin rays, especially proximal to body; pectoral-fin base predominantly brown; anal-fin base predominantly metallic blue-lavender. Underwater photographs of live specimens (Fig. 2): body overall greenish-yellow, less brown and more yellow dorsally, more blue ventrally; caudal peduncle and tail yellow; distal edge of caudal peduncle at junction of posterior dorsal fin with a large white spot, its diameter about width of orbit; pectoral fins yellow, pelvic fins blue; top of orbit and interorbital space yellow; beneath orbit, along cheek and throat blue. Scales on ventral half of body darkened centrally, forming a series of 5–7 faint stripes from behind pectoral fin to caudal-fin base. Occasionally, specimens in underwater photographs taken *in situ* show a second, less-pronounced, smaller, white spot on the body just below the midpoint of the dorsal fin (Fig. 2B).

Coloration of juveniles in life.—(Fig. 2A) Based on color video and photographs of living specimens visualized during Drop-Cam and ROV surveys, juveniles are similar to adults in coloration, but paler overall; body blue to lavender; caudal peduncle and caudal fin yellow; distal edge of caudal peduncle at junction of posterior dorsal fin with a large
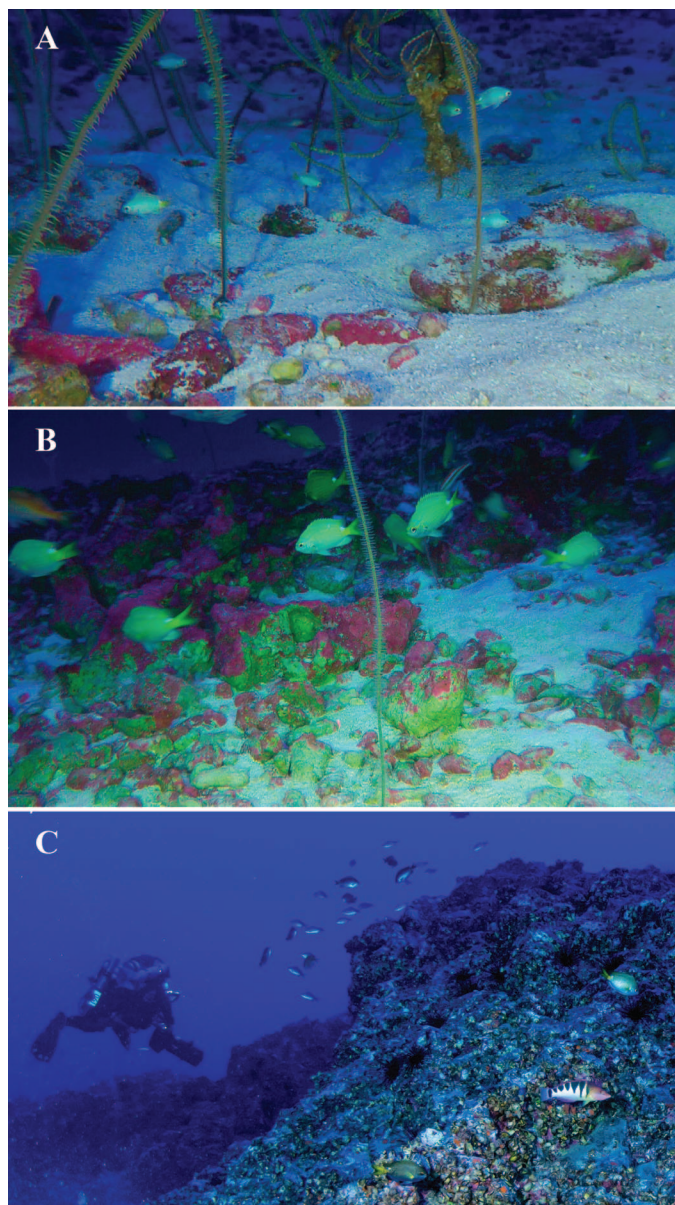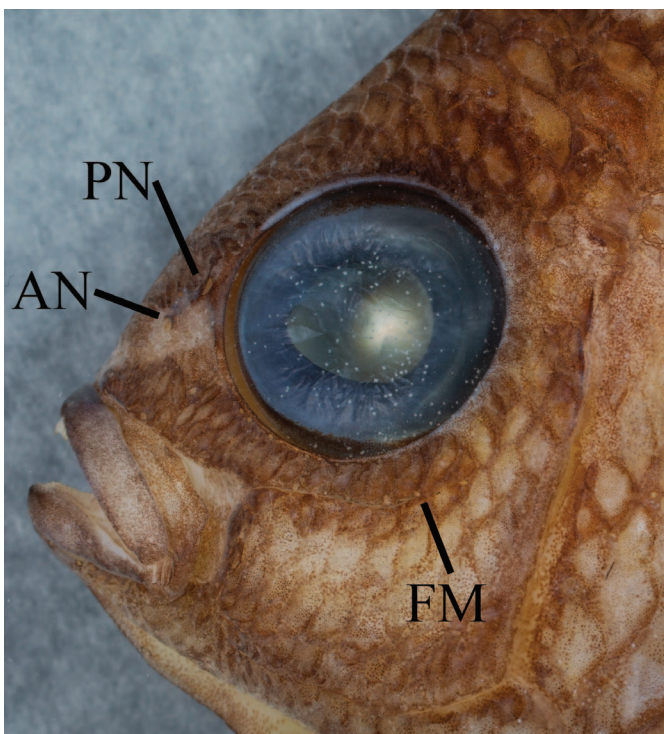
Fig. 2. (A) Aggregation of juvenile *Chromis mamatapara*, new species, in a field of *Stichopathes* sp. whip corals at a depth of 165 m on Pukao. Photo by M. Gorny, Oceana. (B) Aggregation of adult *Chromis mamatapara*, new species, photographed at a depth of 175 m on Pukao. Photo by M. Gorny, Oceana. (C) Collection site of *Chromis mamatapara*, new species, Rapa Nui, Chile, at a depth of 90 m. Two specimens are visible in the foreground, exhibiting the diagnostic white spot at the posterior base of the soft dorsal fin. Associated fishes include *Chaetodon litus*, *Chromis randalli*, *Pseudolabrus semifasciatus*, the recently described *Plectranthias ahiahiata*, *Luzonichthys kiomeamea*, and an undescribed member of the Serranidae. Photo by L. A. Rocha.

Fig. 3. Details of the head of the holotype of *C. mamatapara* showing the preorbital/suborbital scale pattern, anterior nostril (AN), posterior nostril (PN), and posterior edge of the free margin of infraorbital (FM). Photo by J. Fong.

white spot, its diameter about width of orbit; median and paired fins with less yellow than in adults.

Coloration in alcohol.—(Fig. 1B, 1D) Head and body overall straw to light-brown in color, with dark brown pigments retained at base of dorsal fin, upper third of body, on head and at base of median and paired fins; dorsal fin, pelvic fins, and anal fin predominantly brown; posterior margin of caudal fin brown; pectoral fins hyaline distally, pale white proximally.

Habitat and distribution.—*Chromis mamatapara* is only known to occur at Rapa Nui (Easter Island), Isla Salas y Gómez, and the seamount Pukao (∼85 km west of Rapa Nui). Due to the high degree of endemism (21.7%) among the shore fishes of Rapa Nui (Delrieu-Trottin et al., 2019), it is likely that *Chromis mamatapara* is endemic to this region.

The collected fish were recorded at a depth of 90 m in a rocky patch reef surrounded by a large sandy area. Adults have also been observed with ROV surveys at Rapa Nui at 90–230 m and Pukao at 150–190 m in rocky patch reefs surrounded by sandy areas, around rhodoliths and fields of whip coral (*Stichopathes*), along rock walls interspersed with sandy areas, and dead or mostly dead reefs of *Leptoseris*. Juveniles of the new species have been observed during ROV surveys in association with *Stichopathes* at Pukao at 165 m and Rapa Nui at and 150–157 m (Easton et al., 2019; Fig. 2A).

Comparisons.—As with many of its congeners, *Chromis mamatapara* is a wide-bodied planktivorous fish associated with rocky reef structures on MCEs. On the basis of coloration and meristic data, *C. mamatapara* appears to be closely related to several species of *Chromis* bearing 14 dorsal-fin spines, in particular, *C. mirationis, C. okamurai, C. struhsakeri,* and *C. tingting*. The new species also bears resemblance to *C. meridiana, C. notata,* and *C. plansei* in having a pronounced large white spot on the distal edge of the caudal peduncle. Because comparative sequences for several potentially related species of *Chromis* are unavailable, we cannot assess its phylogenetic relationship to all these species. Nonetheless, we compared the sequence data of a fragment of the *COI* gene of *C. mamatapara* to those of all other *Chromis* available in public and our laboratory's databases. *Chromis tingting* (Gen-

Bank accession number MN166324) from Japan has the most similar *COI* sequence (3.5% uncorrected genetic divergence) among these samples (Supplemental Table 1; see Data Accessibility). A second sequence (KU944414) listed in GenBank as *C. okamurai* was a 100% match to the sequence of *C. tingting*, and seems to be a mislabeled specimen of *C. tingting* (Y. K. Tea, pers. comm.).

Most tropical Atlantic species of *Chromis* also possess 14 dorsal spines, but this dorsal-fin formula is less common in the wider Indo-Pacific region (Yamakawa and Randall, 1989; Allen and Erdmann, 2009). Of the valid species of *Chromis*, about 20 of the Indo-Pacific species of *Chromis* possess 14 dorsal spines. Several of these species, including *Chromis mamatapara*, *C. mirationis*, *C. okamurai*, *C. struhsakeri*, and *C. tingting,* are anti-tropical or are found only in MCEs or other deep-water habitats, and share other characters, including two spiniform procurrent caudal-fin rays and an overall grayish-blue coloration with yellow and brown highlights. Tea et al. (2019) summarized this group, highlighting differences in adult coloration, supplementing an initial list provided in Lecchini and Williams (2004) with newly described species. Pyle et al. (2008) proposed a grouping of deep-water *Chromis* characterized by having 14 dorsal-fin spines and low numbers of pectoral-fin rays (18–19) and gill rakers (24–28), to which they assigned *C. abyssus, C. circumaurea, C. degruyi, C. okamurai,* and *C. woodsi*. However, the group of Indo-Pacific *Chromis* with 14 dorsal-fin spines is morphologically diverse and is thus likely polyphyletic (Allen and Erdmann, 2009). As with *Chromis mamatapara,* several species with 14 dorsal-fin spines, including *C. meridiana*, *C. notata*, and *C. planesi*, exhibit a pronounced white spot on the body at the posterior base of the dorsal fin just anterior to the caudal peduncle.

Chromis mamatapara shares a wide suite of morphological characters (14 dorsal-fin spines; 13–14 dorsal-fin rays, 12 anal-fin rays; 18–19 pectoral-fin rays; 8+7 principal caudal-fin rays; 18 tubed lateral-line scales; 11+15 vertebrae; 30–32 total gill rakers) with *C. meridiana, C. mirationis,* and *C. verater*. *Chromis mamatapara* can be distinguished from *C. meridiana* by having a deeper body (depth 50.2–50.9% SL versus 41.8–47.8% SL), a longer snout (6.6–8.7% SL versus 3.6–6.2% SL), and a wider interorbital region (width 10.8–11.0% SL versus 8.7–10.6% SL); from *Chromis mirationis* by having a smaller head (29.5–31.2% SL versus 32.8–35.4% SL), a smaller eye (orbit diameter 9.6–10.8% SL versus 11.4–14.2% SL), a shorter upper jaw (8.5–9.4% SL versus 10.0–12.0% SL), and by lacking a distinct brown stripe extending laterally along the entire length of the midline; from *Chromis verater* by having two (versus three) spiniform procurrent caudal-fin rays, a more pronounced caudal concavity (5.2–7.2 in SL versus 10–14 in SL), and by lacking three smaller white spots located posteriorly at the base of the dorsal, anal, and caudal fins of living specimens.

Etymology.—The specific epithet is a compound word meaning "yellow damselfish" (māmata para) in Rapanui, in reference to the overall body coloration in life. To be treated as a noun in apposition. The suggested English common name, Michel's Chromis (Castañeta de Michel in Spanish), is in honor of the late Michel Garcia, who greatly assisted our field work in Rapa Nui, and unfortunately died in May 2018.

Remarks.—Mesophotic coral ecosystems, popularly known as the coral reef twilight zone, are deeper extensions of the more familiar shallow-water coral reef ecosystems (Rocha et al., 2018; Pyle and Copus, 2019). Because they are outside the range of recreational SCUBA diving, submarines, remotely operated vehicles, baited remote underwater videos, or technical diving using specialized equipment (rebreathers and mixed gases) are needed to explore these deep-reef habitats, complicating and increasing the costs of field operations (Pinheiro et al., 2016; Baldwin et al., 2018). Therefore, relatively little is known about MCEs, and more than 70% of all research at those depths has been published in the past seven years (Pyle and Copus, 2019). As a result, new-species discoveries within MCEs have held a steady high pace over the past two decades (Pyle et al., 2019), and current ichthyological collections are yielding discovery rates as high as two new species per hour of exploration, with new species corresponding to up to 6% of the local biodiversity (Pinheiro et al., 2019a).

Recent studies of MCEs have revealed a dynamic ecology that is prone to shifts in species composition and varied levels of natural disturbances (Rocha et al., 2018; Shepherd et al., 2018b; Pinheiro et al., 2019b). The new species described here, along with two additional recently described species, adds to the high diversity and uniqueness of the fish fauna of Rapa Nui (Shepherd et al., 2018a, 2019). As with many small-range endemics inhabiting these islands, speciation likely occurred following a founder event, supporting the hypothesis that the islands act as an important center of speciation and a cradle of coral reef biodiversity in the region (Delrieu-Trottin et al., 2019). This important evolutionary laboratory should, therefore, be protected by meaningful fishery regulations and conservation management plans that include both shallow coastal reefs and MCEs.

DATA ACCESSIBILITY

Supplemental material is available at https://www.copeiajournal.org/ci-19-294.

ACKNOWLEDGMENTS

LITERATURE CITED

Allen, G. R. 1991. Damselfishes of the World. Mergus, Melle, Germany.

Allen, G. R., and M. V. Erdmann. 2009. Two new species of damselfishes (Pomacentridae: *Chromis*) from Indonesia. aqua, International Journal of Ichthyology 15:121–134.

Allen, G. R., and M. V. Erdmann. 2012. Reef Fishes of the East Indies. Volumes I–III. Tropical Reef Research, Perth, Australia.

Allen, G. R., and J. E. Randall. 2004. Two new species of damselfishes (Pomacentridae: *Chromis*) from Indonesian seas. aqua, Journal of Ichthyology and Aquatic Biology 9: 17–24.

Arango, B. G., H. T. Pinheiro, C. Rocha, B. D. Greene, R. L. Pyle, J. M. Copus, B. Shepherd, and L. A. Rocha. 2019. Three new species of *Chromis* (Teleostei, Pomacentridae) from mesophotic coral ecosystems of the Philippines. ZooKeys 835:1–15.

Baldwin, C. C., L. Tornabene, and D. R. Robertson. 2018. Below the mesophotic. Scientific Reports 8:4920.

Bejarano, I., R. S. Appeldoorn, and M. Nemeth. 2014. Fishes associated with mesophotic coral ecosystems in La Parguera, Puerto Rico. Coral Reefs 33:313–328.

Coleman, R. R., J. M. Copus, D. M. Coffey, R. K. Whitton, and B. W. Bowen. 2018. Shifting reef fish assemblages along a depth gradient in Pohnpei, Micronesia. PeerJ 6: e4650.

Delrieu-Trottin, E., L. Brosseau-Acquaviva, S. Mona, V. Neglia, E. C. Giles, C. Rapu-Edmunds, and P. Saenz-Agudelo. 2019. Understanding the origin of the most isolated endemic reef fish fauna of the Indo-Pacific: coral reef fishes of Rapa Nui. Journal of Biogeography 46:723–733.

Easton, E. E., M. Gorny, A. Mecho, J. Sellanes, C. F. Gaymer, H. L. Spalding, and J. Aburto. 2019. Chile and the Salas y Gómez Ridge, p. 477–490. *In*: Mesophotic Coral Ecosystems. Y. Loya, K. A. Puglise, and T. C. L. Bridge (eds.). Springer, New York.

Easton, E. E., J. Sellanes, C. F. Gaymer, N. Morales, M. Gorny, and E. Berkenpas. 2017. Diversity of deep-sea fishes of the Easter Island ecoregion. Deep-Sea Research Part II: Topical Studies in Oceanography 137:78–88.

Friedlander, A. M., E. Ballesteros, J. Beets, E. Berkenpas, C. F. Gaymer, M. Gorny, and E. Sala. 2013. Effects of isolation and fishing on the marine ecosystems of Easter Island and Salas y Gomez, Chile. Aquatic Conservation: Marine Freshwater Ecosystems 23:515–531.

Kearse, M., R. Moir, A. Wilson, S. Stones-Havas, M. Cheung, S. Sturrock, S. Buxton, A. Cooper, S. Markowitz, C. Duran, T. Thierer, B. Ashton, P. Meintjes, and A. Drummond. 2012. Geneious basic: an integrated and extendable desktop software platform for the organization and analysis of sequence data. Bioinformatics 28:1647–1649.

Lecchini, D., and J. T. Williams. 2004. Description of a new species of damselfish (Pomacentridae: *Chromis*) from Rapa Island, French Polynesia. aqua, Journal of Ichthyology and Aquatic Biology 8:97–102.

Muñoz-Cordovez, R., A. Perez-Matus, L. de la Mesa, and S. A. Carrasco. 2019. Embryonic and larval traits of the temperate damselfish *Chromis crusma* reveals important similarities with other Pomacentridae throughout the family's thermal range. Journal of Fish Biology 95:613–623.

Pinheiro, H. T., G. Eyal, B. Shepherd, and L. A. Rocha. 2019b. Ecological insights from environmental disturbances in mesophotic coral ecosystems. Ecosphere 10:e02666.

Pinheiro, H. T., G. Goodbody-Gringley, M. E. Jessup, B. Shepherd, A. D. Chequer, and L. A. Rocha. 2016. Upper and lower mesophotic coral reef fish communities evaluated by underwater visual censuses in two Caribbean locations. Coral Reefs 35:139–151.

Pinheiro, H. T., B. Shepherd, C. Castillo, R. A. Abesamis, J. M. Copus, R. L. Pyle, B. D. Greene, R. R. Coleman, R. K. Whitton, E. Thillainath, A. A. Bucol, M. Birt, D. Catania, M. V. Bell, and L. A. Rocha. 2019a. Deep reef fishes in the world's epicenter of marine biodiversity. Coral Reefs 38: 985–996.

Pyle, R. L., and J. M. Copus. 2019. Mesophotic coral ecosystems: introduction and overview, p. 3–27. *In*: Mesophotic Coral Ecosystems. Y. Loya, K. A. Puglise, and T. C. L. Bridge (eds.). Springer, New York.

Pyle, R. L., J. L. Earle, and B. D. Greene. 2008. Five new species of the damselfish genus *Chromis* (Perciformes: Labroidei: Pomacentridae) from deep coral reefs in the tropical western Pacific. Zootaxa 1671:3–31.

Pyle, R. L., R. K. Kosaki, H. T. Pinheiro, L. A. Rocha, R. K. Whitton, and J. M. Copus. 2019. Fishes: biodiversity, p. 749–777. *In*: Mesophotic Coral Ecosystems. Y. Loya, K. A. Puglise, and T. C. L. Bridge (eds.). Springer, New York.

Randall, J. E., and A. Cea. 2010. Shore Fishes of Easter Island. University of Hawai'i Press, Honolulu, Hawai'i.

Rocha, L. A., H. T. Pinheiro, B. Shepherd, Y. P. Papastamatiou, O. J. Luiz, R. L. Pyle, and P. Bongaerts. 2018. Mesophotic coral ecosystems are threatened and ecologically distinct from shallow water reefs. Science 361:281–284.

Shepherd, B., T. Phelps, H. Pinheiro, A. Pérez-Matus, and L. Rocha. 2018a. *Plectranthias ahiahiata*, a new species of perchlet from a mesophotic ecosystem at Rapa Nui (Easter Island) (Teleostei, Serranidae, Anthiadinae). ZooKeys 762: 105–116.

Shepherd, B., H. T. Pinheiro, T. Phelps, A. Perez-Matus, and L. A. Rocha. 2019. *Luzonichthys kiomeamea* (Teleostei: Serranidae: Anthiadinae), a new species from a mesophotic coral ecosystem of Rapa Nui (Easter Island). Journal of the Ocean Science Foundation 33:17–27.

Shepherd, B., H. T. Pinheiro, and L. A. Rocha. 2018b. Ephemeral aggregation of the benthic ctenophore *Lyrocteis imperatoris* on a mesophotic coral ecosystem in the Philippines. Bulletin of Marine Science 94:101–102.

Tea, Y. K., A. C. Gill, and H. Senou. 2019. *Chromis tingting*, a new species of damselfish from mesophotic coral ecosystems of southern Japan, with notes on *C. mirationis* Tanaka (Teleostei: Pomacentridae) Zootaxa 4586:249–260.

Thresher, R. E., and P. L. Colin. 1986. Trophic structure, diversity and abundance of fishes of the deep reef (30–300m) at Enewetak, Marshall Islands. Bulletin of Marine Science 38:253–272.

Wieters, E. A., A. Medrano, and A. Perez-Matus. 2014. Functional community structure of shallow hard bottom communities at Easter Island (Rapa Nui). Latin American Journal of Aquatic Research 42:827–844.

Yamakawa, T., and J. E. Randall. 1989. *Chromis okamurai*, a new damselfish from the Okinawa Trough, Japan. Japanese Journal of Ichthyology 36:299–302.